

Scattering Manifestation of Multiferroicity in a Frustrated Magnet

The coexistence of magnetism and ferroelectricity with cross coupling, termed multiferroicity, rarely occurs. Recent discoveries of gigantic magnetoelectric couplings in frustrated magnets offer new opportunities for a thorough scientific understanding of multiferroicity as well as multiferroic applications. With measurements of resonant soft-X-ray magnetic scattering and an analysis based on symmetry considerations, we proffer scattering evidence for multiferroicity and a new pathway for understanding the intricate coupling between magnetism and ferroelectricity in frustrated magnets. The magnetoelectric effect in TbM_2O_5 arises from an internal field determined by $\vec{S}_{\vec{q}} \times \vec{S}_{-\vec{q}}$ with $\vec{S}_{\vec{q}}$ being the magnetization at modulation vector \vec{q} , independent of the commensurability and chirality. Our discoveries set fundamental symmetry constraints on the microscopic mechanism of multiferroicity in frustrated magnets.

Beamline

05B Spin-polarized PES/PEEM

Authors

J. Okamoto, D. J. Huang,
H.-J. Lin, and C. T. Chen
National Synchrotron Radiation
Research Center, Hsinchu,
Taiwan

C. Y. Mou
National Tsing Hua University,
Hsinchu, Taiwan

K. S. Chao
National Chiao-Tung University,
Hsinchu, Taiwan

S. Park and S-W. Cheong
Rutgers University,
Newark, New Jersey, USA



Ever

since it intrigued Greeks, magnetism, in which the ordering of spins comes into play, has kindled great scientific minds. Ferroelectricity is an electronic version of magnetism, associated with the polar arrangement of charges. Technologically, materials with the coexistence of magnetism and ferroelectricity, termed multiferroicity, are attractive because they offer the possibility for realizing mutual control of electric and magnetic properties. The key phenomenon behind such mutual control lies on the capability for the induction of magnetization by an electric field or of electric polarization by a magnetic field, known as the magnetoelectric (ME) effect. The ME effect is an important characterization of multiferroicity but has been poorly understood. The effect could be largely enhanced by the presence of internal fields. However, such enhancement requires the coexistence and strong coupling of magnetism and ferroelectricity (FE), which rarely occur in real materials. Recent discoveries of giant magnetoelectric couplings in frustrated magnets,^[1,2] such as reversibly flipping ferroelectric polarization or drastic change of dielectric constant with applied magnetic fields, thus offer new opportunities for a thorough scientific understanding of multiferroicity as well as multiferroic applications.

In frustrated magnets, such as $RMnO_3$ and RMn_2O_5 ($R = Tb, Dy, \text{ and } Ho$), the spontaneous electric polarization (\vec{P}) appears in certain antiferromagnetic (AF) phases. Unlike old examples of multiferroics, the magnetoelectric couplings exhibited by these materials are gigantic, and the magnetic phases involved are complicated and commonly incommensurate with lattice. The magnetic transition temperature is higher than the ferroelectric one, suggesting that the ferroelectricity is induced by magnetic order. Furthermore, the inversion symmetry in the magnetic phases with ferroelectricity is broken, implying that the magnetic order couples to odd orders of \vec{P} . In addition, these magnets show anomalies in the temperature dependence of dielectric constant ϵ . For $RMnO_3$, the ferroelectric transition is accompanied by a magnetic transition from incommensurate sinusoidal to spiral AF order. Kenzelmann *et al.*^[3] have applied the

Ginzburg-Landau theory to understand the multiferroic behavior. In contrast, although Chapon *et al.*^[4] found that the ferroelectricity in YMn_2O_5 results from acentric spin-density waves, little is known about the underlying mechanism of multiferroicity in RMn_2O_5 because of their structural complexity. The exact relation and interplay between AF order and ferroelectricity in frustrated magnets are unknown and remain controversial.

The presence of internal fields is the simplest origin of the cross coupling between magnetism and ferroelectricity. Microscopically, however, it is difficult to identify them due to their weak effect. Historically, scattering has been shown to be powerful for measuring accumulated microscopic changes and for revealing orderings and their relations directly. Neutron scattering, for example, first convincingly proved the existence of the antiferromagnetic phase of MnO .^[5] Here, by resorting to soft X-ray magnetic scattering and an analysis based on the phenomenological Ginzburg-Landau approach, we demonstrate that the magnetically induced ferroelectricity in TbMn_2O_5 arises from an internal field determined by $\vec{S}_{\vec{q}} \times \vec{S}_{-\vec{q}}$ with $\vec{S}_{\vec{q}}$ being the magnetization at modulation vector \vec{q} . The results indicate that the non-collinearity of spins is essential for the existence of induced \vec{P} , independent of commensurability and chirality. In contrast, the external electric fields alter the exchange coupling, yielding anomalies in the temperature dependence of the dielectric constant.

We present measurements of soft X-ray magnetic scattering around the L_3 ($2p_{3/2} \rightarrow 3d$) absorption edge of Mn to reveal the detailed coupling of ferroelectricity and AF order in TbMn_2O_5 . Soft X-ray magnetic scattering is a newly developed technique which is sensitive to the magnetic moment of transition-metal d electrons, allowing us to probe magnetic order with high sensitivity. The scattering amplitude is proportional to the magnetization $\vec{S}_{\vec{q}}$, which is $\sum_j \vec{S}_j e^{i\vec{q}\cdot\vec{r}}$ with \vec{S}_j and \vec{r} being spin moments and position vectors, respectively. We performed scatter-

ing measurements with the EPU beamline. Figure 1(A) illustrates a schematic view of scattering geometry. A single crystal of $\text{TbMn}_2\text{O}_5(100)$ with dimensions of $2 \times 1 \times 1 \text{ mm}^3$ was cut and polished to achieve a mirror-like surface, followed by a high-temperature annealing to remove built-up strain during polishing. The modulation vector \vec{q} is the momentum transferred from the materials and lies in the scattering plane defined by the a and c axes, i.e., $\vec{q} = (q_a, 0, q_c)$. For photons of 639 eV, the intrinsic q resolution in terms of half width at half maxima (HWHM) is estimated to be of 0.001 \AA^{-1} , including the effect of photon penetration depth. The scattering results reveal that TbMn_2O_5 exhibits an AF order below 42 K. Figure 1 shows the scattering intensity in the $q_a q_c$ plane. To reduce self absorption, we used photons with an energy just below the Mn L_3 edge in the following discussion on the temperature and polarization dependence; for example, the penetration depth ($\sim 1800 \text{ \AA}$) of 639-eV photons is much larger than the correlation length of AF order ($\sim 800 \text{ \AA}$ defined as the inverse of HWHM).

Temperature-dependent measurements indicate that the AF order of TbMn_2O_5 occurs with modulation vectors $(\frac{1}{2} \pm \delta_a, 0, \frac{1}{4} + \delta_c)$, in which δ_a and δ_c characterize the incommensurability. The temperature dependence of q_a is plotted in Fig. 2(A) and Fig. 2(B) for π and σ polarizations, respectively. As the temperature decreases, the incommensurate AF order of TbMn_2O_5 begins to develop at 42 K, in agreement with neutron results. For the temperature between 37 K and 30 K, the incommensurate scattering intensity decreases monotonically; the q_a of the incommensurate ordering moves toward 0.5. In contrast, the commensurate ordering appears between 37 K and 24 K, coexisting with the incommensurate ordering. The scattering intensities plotted in the insets of Fig. 2(A) and Fig. 2(C) demonstrate the coexistence of commensurate and incommensurate AF orderings, similar to the coexistence of commensurate and incommensurate AF

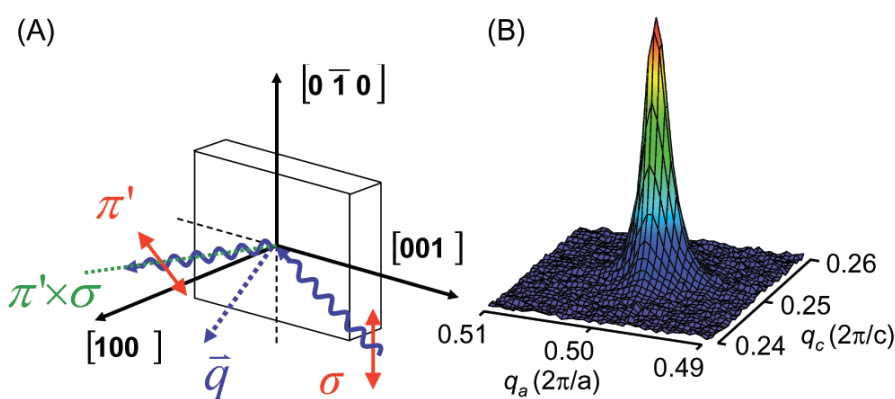


Fig. 1: (A) Schematic view of soft-X-ray scattering measurements on $\text{TbMn}_2\text{O}_5(100)$ with σ and π' polarizations for incident and scattered photons, respectively. With \vec{q} near $(\frac{1}{2}, 0, \frac{1}{4})$, the angle between the scattered X-ray and the a axis is $\sim 6^\circ$ and that between the incident X-ray and the c axis is $\sim 19^\circ$. (B) Scattering intensity plotted in the $q_a q_c$ plane recorded at 30 K with photon energy of 639 eV. The full widths at half maxima (FWHM) of the q_a and q_c scans fitted with a Lorentzian function and a linear background are 0.0020 \AA^{-1} and 0.0025 \AA^{-1} , respectively.

phases observed in YMn_2O_5 . As shown in Fig 3(B), the onset of spontaneous electric polarization is accompanied by the incommensurate-commensurate AF transition at 37 K, contrary to RMnO_3 . On further lowering the temperature, a commensurate-incommensurate transition occurs at 23 K; the commensurate ordering disappears.

The polarization dependence of X-ray scattering provides the information about the direction of magnetic moments. Hannon *et al.*^[6] have shown the magnetic moment along a direction \hat{Z} probed in X-ray scattering is proportional to $(\vec{e}^* \times \vec{e}) \cdot \hat{Z}$, where \vec{e}^* is the electric field of the scattered light. For an incident X-ray of σ polarization,

the scattered X-ray from TbMn_2O_5 with $\vec{e}^* \parallel \hat{b}$ (denoted as σ' polarization) makes no contribution to the magnetic scattering, and the scattered X-ray with $\vec{e}^* \perp \hat{b}$ (π' polarization) is predominantly sensitive to the magnetic moment along the a axis, i.e., $|S_q^a|$, because $(\pi^* \times \sigma)$ is $\sim 6^\circ$ away from the a axis. Conversely, if the incident X-ray has π polarization, the scattered X-ray has either π' or σ' polarization; $(\pi^* \times \pi)$ is parallel to the b axis, whereas $(\sigma^* \times \pi)$ is predominantly along the c direction. As neutron measurements indicate that the magnetic moments are in the ab plane, the scattering with π polarization is predominantly sensitive to the magnetic moment along the b axis, i.e., $|S_q^b|$. Hence the ratio I_σ/I_π of average intensities with σ and π polarization is proportional to $|S_q^a|^2/|S_q^b|^2$.

The knowledge of $|S_q^a|$ and $|S_q^b|$ enables one to investigate how \vec{P} is induced by magnetization based on the Ginzburg-Landau approach. As hinted from the broken inversion symmetry, there must be odd orders of \vec{P} coupling to \vec{S}_q . Clearly, the lowest order coupling is that an internal field \vec{E}_{in} couples to \vec{P} , and the free energy F can be written as $F = P^2/2\chi_0 - \vec{E}_{in} \cdot \vec{P}$ with χ_0 being the electric susceptibility. The minimization of F thus leads to $\vec{P} = \chi_0 \vec{E}_{in}$. From symmetry point of view, because \vec{S}_q changes sign under time reversal, \vec{E}_{in} must be quadratic in magnetization and contains at least two components in \vec{S}_q . Since

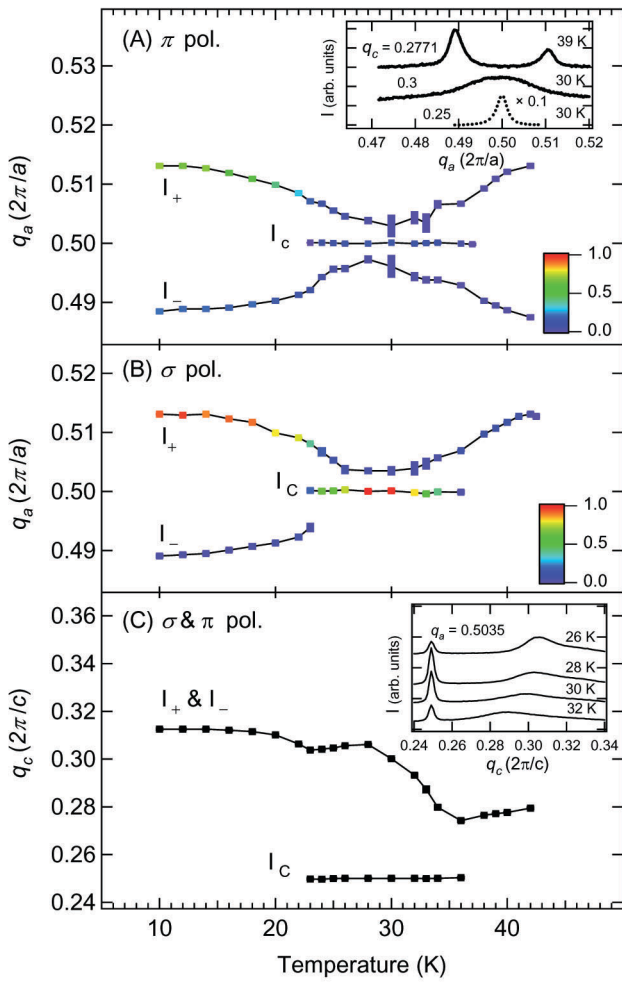


Fig. 2: Temperature-dependent q of AF ordering of TbMn_2O_5 : (A) and (B) q_a component measured with π and σ polarizations; (C) q_c component. The vertical size of rectangular symbols indicates the uncertainty of q_a and q_c . Intensities normalized to that of the commensurate AF ordering at 30 K with polarization are expressed by means of colour. The temperature dependence of q_c is without showing relative intensities. Intensities of incommensurate AF ordering with $\vec{q} = (\frac{1}{2} \pm \delta_a, 0, \frac{1}{4} + \delta_c)$ are denoted as I_{\pm} , and of the commensurate ordering as I_c . The insets of (A) and (C) are, respectively, scattering intensities of q_x and q_z scans at selected temperatures.

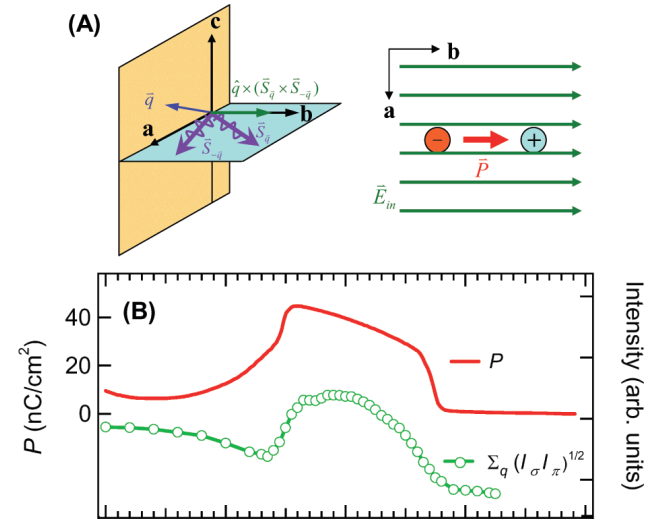


Fig. 3: Graphic illustrations of the symmetry of multiferroicity and ferroelectric properties of TbMn_2O_5 . (A) Left: Cartoon view of the relative orientations of \vec{S}_q and \vec{S}_{-q} . The internal field $\vec{E}_{in} \propto \hat{q} \times (\vec{S}_q \times \vec{S}_{-q})$, where \hat{q} is the unit vector along the direction of \vec{q} . Right: Graphic illustration of \vec{P} induced by \vec{E}_{in} ; (B) Comparison of the polarization P and intensities $\Sigma_q (I_\sigma I_\pi)^{1/2}$. Here, I_σ and I_π are the average intensities for σ and π polarizations, respectively, i.e., $I_{\sigma/\pi} \equiv (I_+ + I_-)/2$ for incommensurate ordering and $I_{\sigma/\pi} \equiv I_c$ for commensurate ordering.

both \bar{q} and $-\bar{q}$ must be paired to make \bar{P} uniform in real space, \bar{E}_{in} must contain both $\bar{S}_{\bar{q}}$ and $\bar{S}_{-\bar{q}}$. Under the inversion operation $\bar{r} \rightarrow -\bar{r}$, $\bar{S}_{\bar{q}}$ becomes $\bar{S}_{-\bar{q}}$. Since \bar{P} changes sign, \bar{E}_{in} must change sign to fulfill F being invariant. Out of the quantities that characterize the magnetic order and the underlying lattice, there are two possible combinations for \bar{E}_{in} : $\hat{u} \times (\bar{S}_{\bar{q}} \times \bar{S}_{-\bar{q}})$ or $(\bar{S}_{\bar{q}} \cdot \bar{S}_{-\bar{q}})\hat{q}$, where \hat{u} is \hat{a} , \hat{b} , \hat{c} or their combinations, representing the most important anisotropic direction in the spin-spin interaction. Since $(\bar{S}_{\bar{q}} \cdot \bar{S}_{-\bar{q}}) = |\bar{S}_{\bar{q}}|^2$ is finite for any magnetic phase occurring below the Neel temperature T_N , an internal field of the form $(\bar{S}_{\bar{q}} \cdot \bar{S}_{-\bar{q}})\hat{q}$ implies that transition temperature for non-vanishing \bar{P} is identical to T_N , which disagrees with experimental observation of TbMn_2O_5 . On the other hand, $\hat{u} \times (\bar{S}_{\bar{q}} \times \bar{S}_{-\bar{q}})$ does discern different magnetic phases. In particular, it vanishes for collinear or inversion-invariant magnetic phases. Therefore, we conclude that $\bar{E}_{\text{in}} = \sum_{\bar{q}} i\gamma_{\bar{q}} \hat{u} \times (\bar{S}_{\bar{q}} \times \bar{S}_{-\bar{q}})$ is the only candidate that is consistent with symmetry considerations for TbMn_2O_5 . Here $\gamma_{\bar{q}}$ is some unknown function to be determined by microscopic models. Then the induced polarization is $\bar{P} = \chi_0 \sum_{\bar{q}} i\gamma_{\bar{q}} \hat{u} \times (\bar{S}_{\bar{q}} \times \bar{S}_{-\bar{q}})$.

For TbMn_2O_5 , because $S_q^c = 0$, by taking $\hat{u} = \hat{q}$, \bar{P} is along the b axis, consistent with experimental observations. The choice of $\hat{u} = \hat{q}$ is also consistent with the work by Mostovoy,^[7] where the proposed expression, after being averaged over space, also shows that \bar{P} is determined by $\bar{S}_{\bar{q}} \times \bar{S}_{-\bar{q}}$. In addition, checking the magnitude of \bar{P} provides another justification. Since $P \propto \sum_{\bar{q}} \gamma_{\bar{q}} |S_{\bar{q}}^a| |S_{\bar{q}}^b| \sin(\phi_a - \phi_b)$ with $\phi_{a/b}$ being phases of $S_{\bar{q}}^{a/b}$, the appearance of \bar{P} requires non-vanishing $\phi_a - \phi_b$, reflecting the requirement of non-collinear spin structure for inducing polarization. Since the change of \bar{q} is small, $\gamma_{\bar{q}}$ is almost temperature-independent. With further assumption of $\phi_a - \phi_b$ being roughly independent of temperature, we have $P \propto \sum_{\bar{q}} (I_{\sigma} I_{\pi})^{1/2}$. Figure 3 shows the comparison of P with the sum of the intensities $(I_{\sigma} I_{\pi})^{1/2}$ over commensurate and incommensurate magnetic orderings. Clearly, they follow each other closely, indicating the validity of the proposed \bar{E}_{in} and the assumption on the temperature independence of $\phi_a - \phi_b$. These observations also indicate that the coexisting incommensurate and commensurate orderings break the inversion symmetry. Furthermore, since \bar{P} is an odd function in any component of $\bar{S}_{\bar{q}}$, strong magnetic fields can simply change the sign of just one component in $\bar{S}_{\bar{q}}$ and result in the observed reversal of \bar{P} in direction.

Experimental Station

Soft X-ray scattering chamber

Publication

J. Okamoto, D. J. Huang, C. Y. Mou, K. S. Chao, H.-J. Lin, S. Park, S-W. Cheong, and C. T. Chen, Phys. Rev. Lett. **98**, 157202 (2007).

References

- T. Kimura et al., Nature **426**, 55 (2003).
- N. Hur et al., Nature **429**, 392 (2004).
- M. Kenzelmann et al., Phys. Rev. Lett. **95**, 087206 (2005).
- L. C. Chapon et al., Phys. Rev. Lett. **96**, 097601 (2006).
- C. G. Shull, W. A. Strauser, and E. O. Wollan, Phys. Rev. **83**, 333 (1951).
- J. P. Hannon, G. T. Trammell, M. Blume, D. Gibbs, Phys. Rev. Lett. **61**, 1241 (1988).
- M. Mostovoy, Phys. Rev. Lett. **96**, 067601 (2006).

Contact E-mail

djhuang@nsrrc.org.tw